Hopf bifurcation and multistability in a system of phase oscillators

Sergey Astakhov[*]
Physics Department, Chair of Radiophysics and Nonlinear Dynamics, Saratov State University, 410012 Saratov, Russia

Naoya Fujiwara[†]
Potsdam Institute for Climate Impact Research (PIK), 14473 Potsdam, Germany

Artem Gulay[‡]
Physics Department, Saratov State University, 410012 Saratov, Russia

Naofumi Tsukamoto
Nuclear Fuel Industries, Ltd., 319-1196 Ibaraki, Japan

Jürgen Kurths
Potsdam Institute for Climate Impact Research (PIK), 14473 Potsdam, Germany;
Institute for Complex Systems Mathematical Biology, University of Aberdeen, Aberdeen, United Kingdom;
and Department of Physics, Humboldt University, 12489 Berlin, Germany

(Received 4 April 2012; revised manuscript received 26 April 2013; published 11 September 2013)

We study the phase reduction of two coupled van der Pol oscillators with asymmetric repulsive coupling under an external harmonic force. We show that the system of two phase oscillators undergoes a Hopf bifurcation and possesses multistability on a 2π-periodic phase plane. We describe the bifurcation mechanisms of formation of multistability in the phase-reduced system and show that the Andronov-Hopf bifurcation in the phase-reduced system is not an artifact of the reduction approach but, indeed, has its prototype in the nonreduced system. The bifurcational mechanisms presented in the paper enable one to describe synchronization effects in a wide class of interacting systems with repulsive coupling e.g., genetic oscillators.

DOI: 10.1103/PhysRevE.88.032908 PACS number(s): 05.45.Xt

I. INTRODUCTION

Synchronization phenomena are one of the highlights of nonlinear dynamics [1,2]. There exist many examples in the real world: mechanics [3], electronics [4], biology [5], neuroscience [6,7], chemistry [8,9], Earth sciences [10–12], economics [13], sociology [14], etc. Synchronization can be observed for different types of oscillations and studied in various models. Coupled phase-reduced oscillators are studied intensively both theoretically [1,15–19] and experimentally [20,21]. For chaotic systems, various types of synchronization have been reported [22–25]. Synchronization in complex networks has also been intensively studied [26–33].

Despite its importance, e.g., its applications to brain science [34], there have been only a very few studies on quasiperiodic oscillators. Recently, the problem of the bifurcation scenario for synchronization of quasiperiodic oscillators has been considered [35–38]. A model system of two coupled van der Pol oscillators under external harmonic force has been treated using the phase reduction approach [37]. It has been shown that the synchronization route in the initial system is based on a tangency bifurcation of closed invariant curves. This bifurcation corresponds to a saddle-node bifurcation of two-dimensional invariant ergodic tori in the phase space of the nonreduced system [38]. Here we consider the same system as in Ref. [37], which is a two-dimensional system of phase oscillators with a simple coupling term. This model can be obtained by the phase reduction of two van der Pol oscillators under an external harmonic forcing. In contrast to [37], we introduce an asymmetrical repulsive coupling into the system of interacting oscillators in the present paper. We show that the use of asymmetrical repulsive coupling leads to the emergence of an Andronov-Hopf bifurcation and the formation of multistability in the system of phase equations. The Andronov-Hopf bifurcation in systems of phase oscillators has been reported before [18,19]. However, this bifurcation was observed in a system of Kuramoto phase oscillators characterized by phase space dimension >2 and a complex coupling. Moreover, it has not been shown whether there exists a prototype of this bifurcation in a nonreduced system or it is typical only for abstract phase models. Here we show that the Andronov-Hopf bifurcation in the phase oscillator system indeed corresponds to a bifurcation in the initial nonreduced system of coupled van der Pol oscillators under external harmonic forcing.

Also, we would like to note that the asymmetric repulsive coupling considered here has not been studied much [39,40] despite its importance in systems, e.g., synthetic genetic circuits [41–43]. Our contribution also sheds light on understanding phenomena observed in repulsively coupled interacting systems, e.g., the coexistence of different synchronization regimes.

[*]s.v.astakhov@gmail.com
[†]Present address: FIRST, Aihara Innovative Mathematical Modelling Project, Japan Science and Technology Agency, and Institute of Industrial Science, The University of Tokyo, 153-8505 Tokyo, Japan; fujiwara@sat.t.u-tokyo.ac.jp
[‡]gulai.artem@gmail.com

 ©2013 American Physical Society

The paper has the following structure. In Sec. II we describe the system under study and derive analytically the conditions for an Andronov-Hopf bifurcation. In Sec. III we carry out a bifurcational analysis of the system and show the evolution of the phase-space structure when control parameters are varied. In Sec. IV we draw parallels between the Andronov-Hopf bifurcation in the phase-reduced system and its prototype in the nonreduced system of van der Pol oscillators. In Sec. V we discuss the obtained results.

II. SYSTEM UNDER STUDY

We choose a system of two asymmetrically coupled van der Pol oscillators under external harmonic force as a prototype:

$$\begin{aligned}\ddot{x}_1 - \varepsilon\left(1-x_1^2\right)\dot{x}_1 + \omega_1^2 x_1 &= \gamma_1\left(\dot{x}_2 - \dot{x}_1\right) + C_0\cos(\omega_0 t),\\ \ddot{x}_2 - \varepsilon\left(1-x_2^2\right)\dot{x}_2 + \omega_2^2 x_2 &= \gamma_2\left(\dot{x}_1 - \dot{x}_2\right).\end{aligned} \tag{1}$$

Here $x_{1,2}$ are the dynamical variables, ε is the nonlinearity parameter, $\omega_{1,2}$ are the natural frequencies of the partial oscillators, $\gamma_{1,2}$ are the coupling coefficients, and C_0 and ω_0 are the amplitude and the frequency of the external force, respectively. Using the standard procedure of quasiharmonic approximation [2],

$$x_1 = a_1(t)\cos\left(\omega_0 t + \varphi_1(t)\right), \quad x_2 = a_2(t)\cos\left(\omega_0 t + \varphi_2(t)\right),$$

one can easily obtain a phase-reduced model for (1):

$$\begin{aligned}\dot{\varphi}_1 &= \Delta_1 + g_1\sin(\varphi_2 - \varphi_1) - \frac{C}{1-\Delta_1}\cos\varphi_1,\\ \dot{\varphi}_2 &= \Delta_1 + \delta - g_2\sin(\varphi_2 - \varphi_1).\end{aligned} \tag{2}$$

Here $\varphi_{1,2}$ denote the phase difference between the external harmonic force of the first and second van der Pol oscillators in (1), respectively; $g_{1,2} = \gamma_{1,2}/2$ are the coupling coefficients; and $\Delta_{1,2} = (\omega_{1,2}^2 - \omega_0^2)/(2\omega_0)$, $\delta = \Delta_2 - \Delta_1$, $C = C_0/(2a_1)$. In the framework of the phase reduction we assume $a_{1,2} \equiv$ const. The model system, (2), has four equilibrium states:

$$\begin{aligned}\varphi_1^{(1)} &= \arccos\left[\frac{1-\Delta_1}{C}\left(\Delta_1 + \frac{g_1}{g_2}(\Delta_1+\delta)\right)\right],\\ \varphi_2^{(1)} &= \varphi_1^{(1)} + \arcsin\left(\frac{\Delta_1+\delta}{g_2}\right);\end{aligned} \tag{3a}$$

$$\begin{aligned}\varphi_1^{(2)} &= \arccos\left[\frac{1-\Delta_1}{C}\left(\Delta_1 + \frac{g_1}{g_2}(\Delta_1+\delta)\right)\right],\\ \varphi_2^{(2)} &= \varphi_1^{(2)} - \arcsin\left(\frac{\Delta_1+\delta}{g_2}\right) + \pi;\end{aligned} \tag{3b}$$

$$\begin{aligned}\varphi_1^{(3)} &= -\arccos\left[\frac{1-\Delta_1}{C}\left(\Delta_1 + \frac{g_1}{g_2}(\Delta_1+\delta)\right)\right],\\ \varphi_2^{(3)} &= \varphi_1^{(3)} + \arcsin\left(\frac{\Delta_1+\delta}{g_2}\right);\end{aligned} \tag{3c}$$

$$\begin{aligned}\varphi_1^{(4)} &= -\arccos\left[\frac{1-\Delta_1}{C}\left(\Delta_1 + \frac{g_1}{g_2}(\Delta_1+\delta)\right)\right],\\ \varphi_2^{(4)} &= \varphi_1^{(4)} - \arcsin\left(\frac{\Delta_1+\delta}{g_2}\right) + \pi.\end{aligned} \tag{3d}$$

Here superscripts denote the corresponding fixed points. These equilibrium states exist in the region where the following conditions are satisfied:

$$\begin{aligned}\left|\frac{1-\Delta_1}{C}\left(\Delta_1 + \frac{g_1}{g_2}(\Delta_1+\delta)\right)\right| &\leqslant 1,\\ \left|\frac{\Delta_1+\delta}{g_2}\right| &\leqslant 1.\end{aligned} \tag{4}$$

To analyze the stability of the equilibria, we derive the corresponding eigenvalues of the Jacobian matrix for (2):

$$\begin{aligned}\lambda_j^{(i)} = \frac{1}{2}\Bigg\{ &-\left((g_1+g_2)\cos\left(\varphi_2^{(i)} - \varphi_1^{(i)}\right) - \frac{C}{1-\Delta_1}\sin\varphi_1^{(i)}\right)\\ &-(-1)^j\Bigg[\left((g_1+g_2)\cos\left(\varphi_2^{(i)} - \varphi_1^{(i)}\right) - \frac{C}{1-\Delta_1}\sin\varphi_1^{(i)}\right)^2\\ &+4g_2\frac{C}{1-\Delta_1}\cos\left(\varphi_2^{(i)} - \varphi_1^{(i)}\right)\sin\varphi_1^{(i)}\Bigg]^{\frac{1}{2}}\Bigg\},\\ i = 1,2,3,4, \quad &j = 1,2.\end{aligned} \tag{5}$$

The obtained formula implies complex values of λ when the expression in the square brackets in (5) is negative. In this case the corresponding equilibrium points are foci. It should be noted that the formula for eigenvalues in Ref. [37] is the same, but only for $g_1 = g_2 > 0$. Therefore the steady states of the model system considered in [37] can have only real eigenvalues and can, therefore, be nodes or saddles only.

Complex eigenvalues, (5) provide, the possibility of an Andronov-Hopf bifurcation when the real part

$$(g_1+g_2)\cos\left(\varphi_2^{(i)} - \varphi_1^{(i)}\right) - \frac{C}{1-\Delta_1}\sin\varphi_1^{(i)}$$

of an eigenvalue changes its sign, while the imaginary part remains nonzero. Keeping in mind these requirements, one can derive necessary conditions for the appearance of an Andronov-Hopf bifurcation in (2):

$$\begin{aligned}\left|\frac{1-\Delta_1}{C}\left(\Delta_1 + \frac{g_1}{g_2}(\Delta_1+\delta)\right)\right| &\leqslant 1,\\ \left|\frac{\Delta_1+\delta}{g_2}\right| &\leqslant 1,\\ g_2(g_1+g_2) &< 0.\end{aligned} \tag{6}$$

Here, the first and second lines provide the existence of equilibrium points, while the third line provides the nonzero imaginary part of the eigenvalues, (5).

The known scenario of synchronization of quasiperiodic oscillations in the phase approach originally described in Ref. [37] does not include a Hopf bifurcation because the eigenvalues of the steady states can never be complex in that case. Indeed, usually the Hopf bifurcation arises in the synchronization scenario, when a model system is treated with the amplitude-phase approach and it corresponds to the "suppression" scenario of synchronization. Then the Hopf bifurcation corresponds to the Neimark-Sacker bifurcation in the nonreduced system, which is characterized by the emergence of a torus in the vicinity of a limit cycle. However, in our case we are restricted by the phase approach and the Hopf bifurcation leads to a regime where the phase variables do not increase constantly but oscillate in certain intervals, while the amplitude variables are treated as constant.

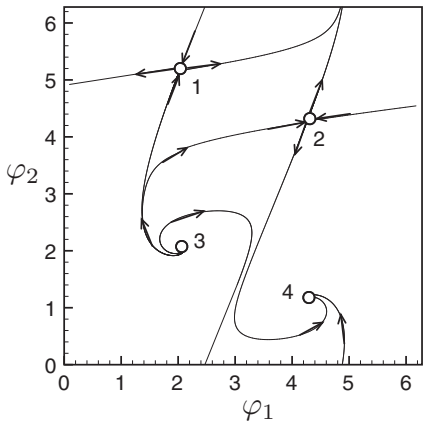

FIG. 1. Phase-space structure of system (2) for $\Delta_1 = -0.1$, $C = 0.25$, $\delta = 0.1$, $g_1 = 0.15$, $g_2 = -0.0616$: 1 and 2 are saddle equilibrium states, 3 is an unstable focus, and 4 is a stable focus.

III. BIFURCATION ANALYSIS

Now we analyze the phase-space structure evolution for the model system, (2), with the control parameters satisfying conditions, (6). We start from the following values of the control parameters: $\Delta_1 = -0.1$, $C = 0.25$, $\delta = 0.1$, $g_1 = 0.15$, $g_2 = -0.0616$. The phase space of the considered system has a structure presented in Fig. 1 (to obtain the phase portraits we have developed our own code in C++, programming language using the fourth-order Runge-Kutta method to integrate the differential equations). As one can see in the figure, the system of phase oscillators, (2), has four fixed points. The situation is similar to the case considered in [37], however, here we have two foci (denoted 3 and 4 in Fig. 1) instead of two nodes.

Now let us vary the parameter Δ_1. The corresponding phase-space structure evolution is presented in Fig. 2. With an increment in Δ_1, pairs of the fixed points approach each other and the imaginary parts of their eigenvalues approach 0. At $\Delta_1 = -0.0431$ the eigenvalues become real and the foci become nodes [Fig. 2(a)]. A further increase in Δ_1 leads to pairwise saddle-node bifurcations of the fixed points at $\Delta_1 = -0.0383$ [Fig. 2(b)]. As a result of the saddle-node bifurcation, two invariant closed curves appear in the phase space: a stable [denoted C_s in Fig. 2(b)] and an unstable [denoted C_u in Fig. 2(b)] curve. These two curves approach each other as Δ_1 increases, and at $\Delta_1 = 0.383$ a tangency bifurcation of C_u and C_s takes place. As a result, the phase trajectory covers the phase plane densely [Fig. 2(c)]. If we decrease Δ_1 starting from $\Delta_1 = -0.1$, the scenario shown in Fig. 3 is observed. It is clearly shown that the bifurcation scenario is similar to the one presented in Fig. 2.

A one-parametric bifurcation diagram for the observed case is constructed and presented in Fig. 4. A phase-parametric diagram for region B is presented in Fig. 5 (we have used

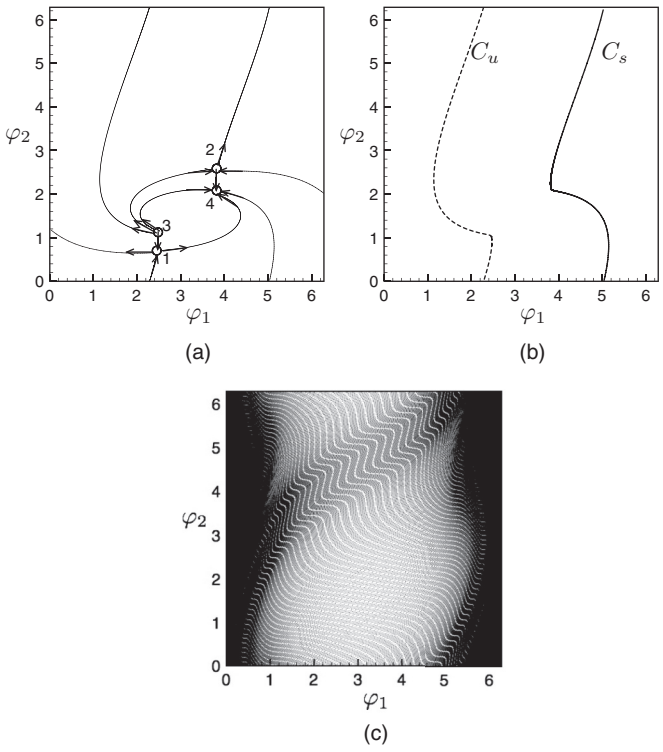

FIG. 2. Phase-space structure evolution for system (2) with $C = 0.25$, $\delta = 0.1$, $g_1 = 0.15$, $g_2 = -0.0616$. (a) $\Delta_1 = -0.04$; foci become nodes. (b) $\Delta_1 = -0.0383$, fixed points undergo pairwise saddle-node bifurcations, and two closed invariant curves (stable, C_s, and unstable, C_u) appear as the result. (c) $\Delta_1 = 0.438$; closed invariant curves undergo tangency bifurcation, and the phase trajectory densely covers the 2π-periodic phase plane.

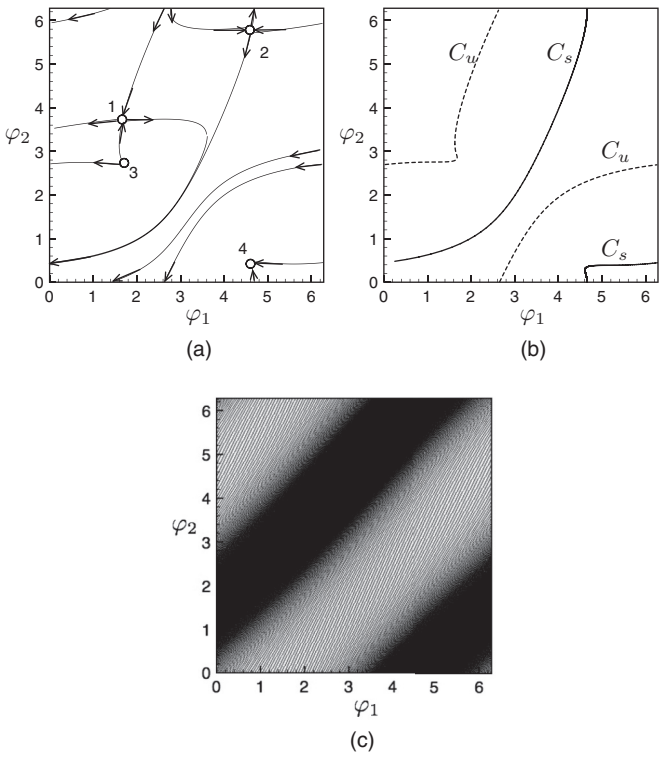

FIG. 3. Phase-space structure evolution for system (2) with $C = 0.25$, $\delta = 0.1$, $g_1 = 0.15$, $g_2 = -0.0616$. (a) $\Delta_1 = -0.155$; foci become nodes. (b) $\Delta_1 = -0.162$; fixed points undergo pairwise saddle-node bifurcations, and two closed invariant curves (stable, C_s, and unstable, C_u) appear as the result. (c) $\Delta_1 = -1.5$; closed invariant curves undergo tangency bifurcation, and the phase trajectory densely covers the 2π-periodic phase plane.

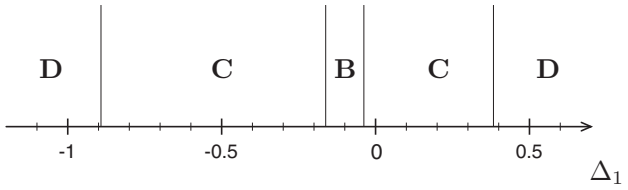

FIG. 4. One-parametric bifurcation diagram for system (2) with $C = 0.25$, $\delta = 0.1$, $g_1 = 0.15$, $g_2 = -0.0616$. Region B corresponds to the structure presented in Fig. 1: there are four equilibrium states:– two foci and two saddles. Region C corresponds to the situation presented in Figs. 2(a) and 3(a). Region D corresponds to the structure observed in Figs. 2(c) and 3(c).

the XPPAUT package [44] to calculate the phase-parametric diagrams). The observed bifurcations are similar to the case considered in [37]. However, there is one important difference: we have obtained two foci in system (2).

Now we decrease the value of the parameter C and set the following values of control parameters: $\Delta_1 = -0.1$, $C = 0.15$, $\delta = 0.1$, $g_1 = 0.15$, $g_2 = -0.0616$. For this case the phase-space structure is presented in Fig. 6. The situation is very different from the one shown in Fig. 1. Besides the four equilibrium points, there are two invariant closed curves, C_s and C_u, of the type shown in Figs. 2(b) and 3(b) (we denote them as invariant closed curves of type I) and two closed curves, C_s^* and C_u^*, of a new type (which we denote type II). Unlike the invariant closed curves observed in [37] (which are all of type I in our classification), these curves do not cross the phase plane in any direction and the coordinates of the phase point on the curve oscillate. The dynamics on such a closed curve resembles the dynamics of a limit cycle.

The observed type of phase-space structure implies a multistability phenomenon of periodic solutions. Indeed, three stable regimes coexist for the given set of control parameters. There is a stable focus 4 separated from the stable type I invariant closed curve C_s by the type II unstable invariant closed curve C_u^* and a type II stable invariant closed curve

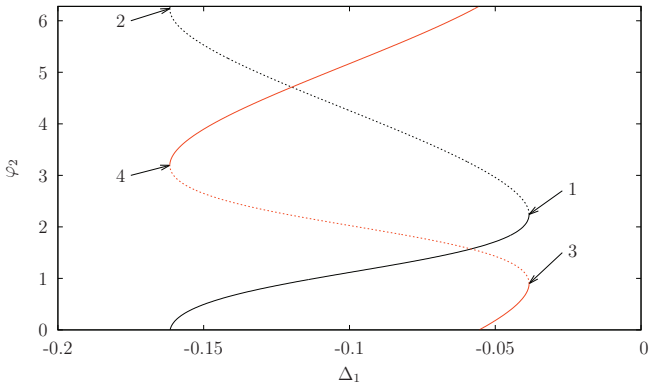

FIG. 5. (Color online) Phase-parametric diagram for system (2) with $C = 0.25$, $\delta = 0.1$, $g_1 = 0.15$, $g_2 = -0.0616$. The solid black curve denotes a stable equilibrium; dashed curves denote saddles; the solid gray (red) curve denotes the repeller. 1 and 2 denote saddle-node bifurcations of equilibria 2 and 4 [see Figs. 2(a) and 3(a)]; 3 and 4 denote saddle-repeller bifurcations of equilibria 1 and 3 (see the same figures).

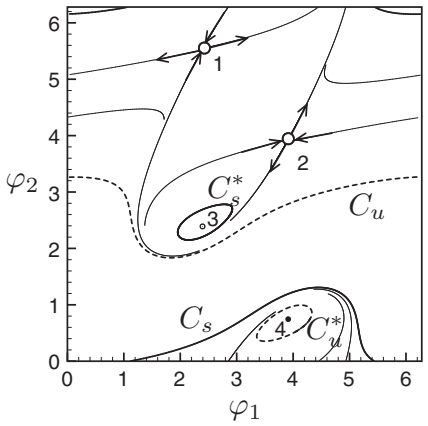

FIG. 6. Phase-space structure of system (2) for $\Delta_1 = -0.1$, $C = 0.15$, $\delta = 0.1$, $g_1 = 0.15$, $g_2 = -0.0616$. 1 and 2 are saddle equilibrium points; 3 and 4 are unstable and stable foci, respectively; C_u and C_s are unstable and stable invariant closed curves of type I, respectively; and C_s^* and C_u^* are stable and unstable closed invariant curves of type II, respectively.

C_s^* separated from the type I stable invariant closed curve C_s by the unstable type I invariant closed curve C_u and by the invariant manifolds of saddles 1 and 2.

To explain the mechanisms of formation of the observed structure, we vary the parameter Δ_1. The phase-space structure evolution when Δ_1 is increasing is presented in Fig. 7. An increment of Δ_1 leads to a reduction in the C_s^* and C_u^* radii, and at $\Delta_1 = -0.097$ a Hopf bifurcation takes place [type II closed invariant curves disappear in the vicinity of the foci and the foci change their stability; see Fig. 7(a)]. A further increment of Δ_1 leads to a reduction in the imaginary parts of the eigenvalues of the foci when the foci approach the saddles. At $\Delta_1 = -0.073$ the foci become nodes as the imaginary parts of their eigenvalues vanish [see Fig. 7(b)]. It has to be noted that the structure of the phase space is different from the case presented in Figs. 2(a) and 3(a), because there are invariant closed curves, C_s and C_u, which coexist with the equilibrium points. After a saddle-node bifurcation at $\Delta_1 = -0.072$, the equilibrium points disappear and only the type I invariant closed curves C_s and C_u remain in the phase space [see Fig. 7(c)]. A further increment of Δ_1 leads to a tangency bifurcation of C_s and C_u at $\Delta_1 = 0.134$ and the phase trajectory covers the phase space densely [see Fig. 7(d)].

Variation of Δ_1 in the negative direction leads to the phase-space structure evolution presented in Fig. 8. As one can see, the situation here is similar to the one presented in Fig. 7 except for the bifurcation illustrated in Fig. 8(a). Here both C_s^* and C_u approach the homoclinic loop of the saddle equilibrium point 2 and at $\Delta_1 = -0.109$ the tangency of these three limit sets takes place. The same situation is observed for C_u^*, C_s, and the homoclinic loop of saddle 1. The observed evolution of the phase-space structure enabled us to construct the one-parametric bifurcation diagram presented in Fig. 9. The phase-parametric bifurcation diagram of regions A and B is presented in Fig. 10.

The Andronov-Hopf bifurcation found in the phase oscillator system, (2), is robust and can be observed in the

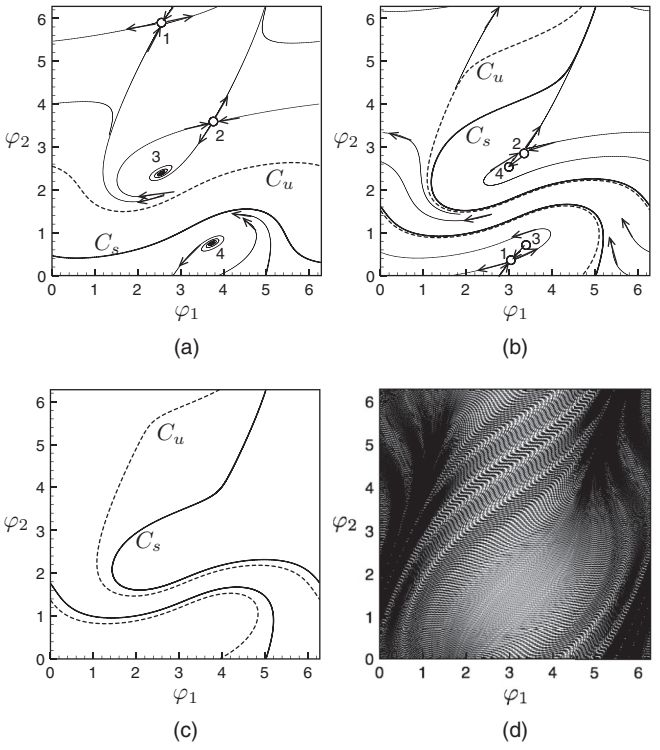

FIG. 7. Phase-space structure evolution of system (2) for $C = 0.15$, $\delta = 0.1$, $g_1 = 0.15$, $g_2 = -0.0616$. (a) $\Delta_1 = -0.09$; the limit cycles C_s^* and C_u^* have reduced around foci 3 and 4, respectively, and disappeared through the Hopf bifurcation at $\Delta_1 = -0.097$. (b) $\Delta_1 = -0.073$; foci 3 and 4 become nodes and approach saddles 1 and 2, respectively. (c) $\Delta_1 = -0.072$; pairwise saddle-node bifurcations take place. (d) $\Delta_1 = 0.18$; invariant closed curves C_s and C_u disappear after the tangency bifurcation at $\Delta_1 = 0.134$.

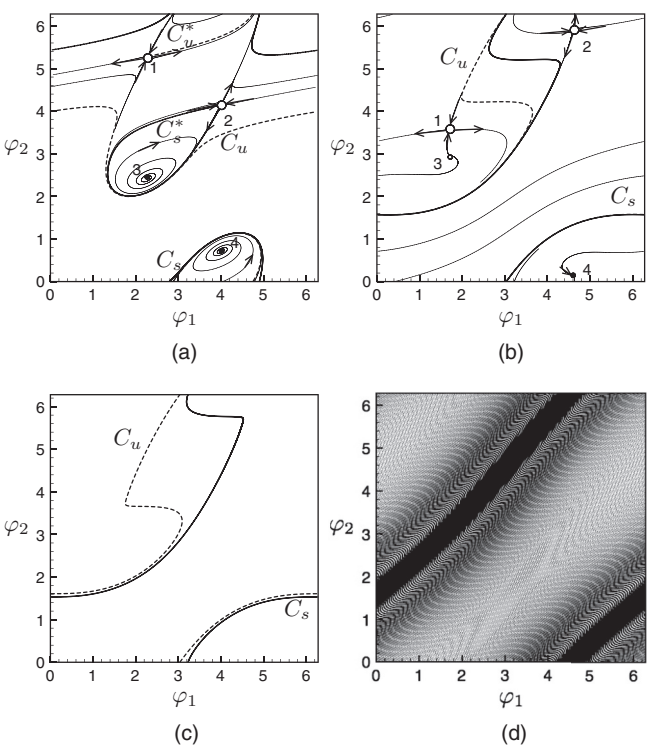

FIG. 8. Phase-space structure evolution of system (2) for $C = 0.15$, $\delta = 0.1$, $g_1 = 0.15$, $g_2 = -0.0616$. (a) $\Delta_1 = -0.109$. (b) $\Delta_1 = -0.159$; foci 3 and 4 become nodes and approach saddles 1 and 2, respectively. (c) $\Delta_1 = -0.162$; pairwise saddle-node bifurcations take place. (d) $\Delta_1 = -0.7$; invariant closed curves C_s and C_u disappear after the tangency bifurcation at $\Delta_1 = -0.526$.

system, not just for the chosen values of control parameters. Figure 11 shows bifurcation lines of the Hopf bifurcation and of the tangency bifurcation on the parameter plane of (g_1, g_2), indicating that the observed phenomena occur over a wide range of coupling strengths. The corresponding structures in the phase space are presented in Fig. 12.

IV. COMPARISON TO THE NONREDUCED CASE

From the bifurcational analysis of the phase oscillator system, (2), we obtained the following results. In the region of existence of equilibrium states on the control parameter plane (Δ, C) two types of bifurcations of the steady states can be realized: a saddle-node bifurcation and an Andronov-Hopf bifurcation. The lines corresponding to the saddle-node bifurcation restrict the region of existence of the equilibrium points. This region corresponds to a so-called Arnold's tongue in the nonreduced system, (1), where oscillations are synchronized on a single frequency [2]. However, the Andronov-Hopf bifurcation in the reduced system, (2), is of special interest. We have explicitly shown that this bifurcation can be realized in (2) only in the case of nonsymmetric repulsive coupling, (6). The corresponding bifurcational transitions in (1) have not been analyzed yet. Hence, the following question arises: Is the Andronov-Hopf bifurcation in the phase oscillators an artifact of the reduction method? In other words, does it correspond to any bifurcation in the nonreduced system?

To answer this question we consider the nonreduced system, (1), with the same values of the control parameters as in the case of the phase oscillators, (2). The Hopf bifurcation of equilibrium point 3 in the phase oscillator system, (2), is presented in Fig. 13(a). To compare the behavior of the nonreduced system of van der Pol oscillators under an external harmonic force, (1), with the dynamics of the phase oscillators, (2), we use the stroboscopic section with the

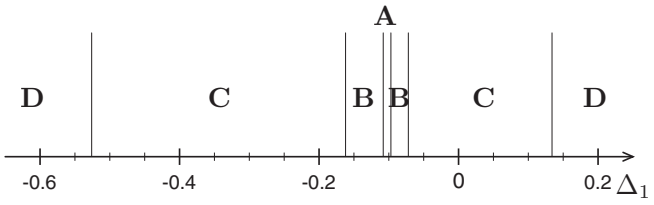

FIG. 9. One-parametric bifurcation diagram for system (2) with $C = 0.15$, $\delta = 0.1$, $g_1 = 0.15$, $g_2 = -0.0616$. Region A corresponds to the structure presented in Fig. 6: there are four equilibrium states, two invariant closed curves of type I, and two invariant closed curves of type II. Region B corresponds to the structure presented in Figs. 7(b) and 8(b). Region C corresponds to Figs. 7(c) and 8(c). Region D corresponds to Figs. 7(d) and 8(d). Regions B, C, and D show qualitatively the same phase-space structures as the ones in Fig. 4.

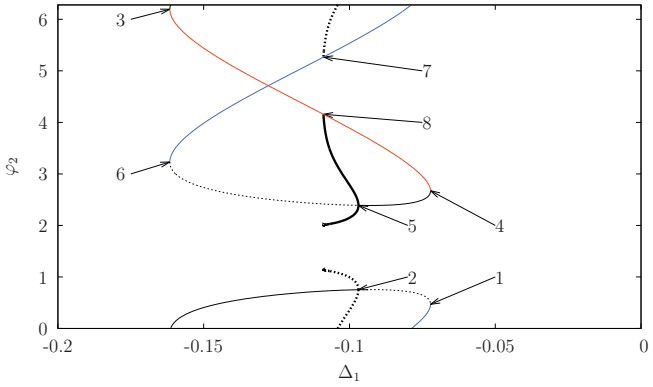

FIG. 10. (Color online) Phase-parametric diagram for system (2) with $C = 0.15$, $\delta = 0.1$, $g_1 = 0.15$, $g_2 = -0.0616$. The thin solid black curve denotes a stable equilibrium; the thin dashed curves denote unstable equilibria; the solid gray (red and blue) curves denote saddles. The thick solid black curve denotes C_s^*; the thick dashed black curve denotes C_u^*. 1, 3, 4, and 6 denote a saddle-node bifurcation [see Figs. 7(b) and 8(b)]; 2 and 5 denote Hopf bifurcations; 7 and 8 denote tangency bifurcations of closed invariant curves with the homoclinic loops of saddles.

period $T = 2\pi/\omega_0$ of the external forcing and the following coordinate transformation:

$$\psi_1 = -\arctan\left(\frac{y_1}{x_1}\right), \quad \psi_2 = -\arctan\left(\frac{y_2}{x_2}\right). \qquad (7)$$

The results are presented in Fig. 13(b). A comparison of the results presented in Figs. 13(a) and 13(b) clearly shows that the Andronov-Hopf bifurcation found in the phase-reduced system, (2), is not an artifact of the reduction routine but is indeed observed in the nonreduced system (1).

Hence, the Andronov-Hopf bifurcation in the phase-reduced system, (2), corresponds to the emergence of a two-dimensional invariant torus [see Fig. 13(c)] in the nonreduced system, (1). This corresponds to a Neimark-Sacker bifurcation, however, here we deal with an unusual case. Usually, a Neimark-Sacker bifurcation corresponds to an Andronov-Hopf bifurcation in a reduced system including amplitude and phase equations. Indeed, the torus appearing as the result of the Neimark-Sacker bifurcation describes amplitude-modulated oscillations in the nonreduced system. In our case we are restricted by phase equations considering the amplitudes as constants. However, taking into account that (2) is a two-dimensional dynamical system the phase differences between the phases of each oscillator in (1) and the external forcing can oscillate. Therefore the two-dimensional torus 2′ in Fig. 13(c) is an image of phase-modulated oscillations.

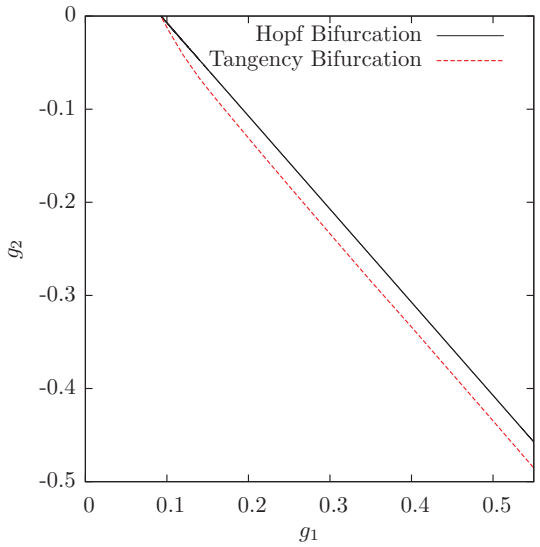

FIG. 11. (Color online) Bifurcation diagram for the phase-reduced system, (2), on the (g_1, g_2) parametric plane for $C = 0.15$, $\delta = 0.1$, $\Delta_1 = -0.1$. The solid line denotes an Andronov-Hopf bifurcation and the dashed (red) line denotes the tangency bifurcation of the limit cycle and the homoclinic loop of the saddle.

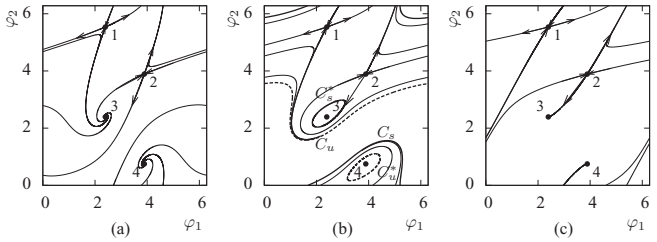

FIG. 12. Structure of the phase space of the phase-reduced system, (2), for $C = 0.15$, $\delta = 0.1$, $\Delta_1 = -0.1$, $g_2 = -0.1$, and (a) $g_1 = 0.1$, (b) $g_1 = 0.185$, and (c) $g_1 = 0.3$. 1 and 2 are saddles, 3 and 4 are foci, $C_{s,u}$ are type I invariant closed curves, and $C_{s,u}^*$ are type II closed invariant curves.

V. SUMMARY AND DISCUSSION

In this paper we have considered a system of phase equations which was obtained using the phase reduction approach applied to a system of two van der Pol oscillators with asymmetric repulsive coupling under external excitation, (1).

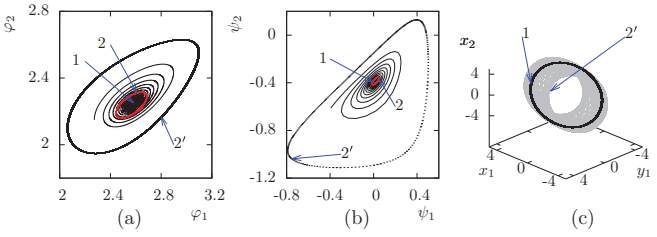

FIG. 13. (Color online) The Andronov-Hopf bifurcation in (2), with $\Delta_1 = -0.08$, $g_1 = 0.15$, $g_2 = -0.0616$, and $\delta = 0.1$, and the corresponding torus emergence in the nonreduced system, (1). (a) Before the bifurcation ($C = 0.16$) the reduced system, (2), possesses the stable focus 1 on the phase plane. A similar focus can be observed in the stroboscopic section of the nonreduced system, (1), in coordinates, (7). (c) This regime corresponds to the stable limit cycle 1 in the phase space of the nonreduced system, (1). After the bifurcation ($C = 0.1659$) the stable limit cycle 2 appears in the reduced system, (2) (a), as well as in the stroboscopic section of (1) (b). Further increase in the control parameter leads to an increase in the limit cycle both in the reduced system, (2), and in the stroboscopic section of (1). The limit cycle for $C = 0.17$ is denoted 2′ in (a) and (b). In the nonreduced system, (1), 2′ corresponds to a two-dimensional torus.

We have shown that the use of asymmetrical repulsive coupling between oscillators leads to a new synchronization scenario. Using the phase reduction approach we obtained a system of two phase oscillators with a simple coupling term where an Andronov-Hopf bifurcation is realized. This bifurcation was observed before in a system of Kuramoto oscillators with higher dimension and complex coupling [18,19]. However, this bifurcation in this type of system has been studied rarely and it was not clear whether it has a prototype in a nonreduced real-world system. In this paper we have shown that the Andronov-Hopf bifurcation in the phase reduction corresponds to the emergence of a two-dimensional torus on the basis of a limit cycle (the Neimark-Sacker bifurcation) which is the image of phase-modulated oscillations in the nonreduced system.

A necessary condition for an Andronov-Hopf bifurcation is negativeness of one of the coupling coefficients, which means that the coupling must be repulsive and asymmetric. Nowadays, the role of repulsive coupling is attracting the attention of researchers in different branches of nonlinear science. We show that in the reduced system the Hopf bifurcation leads to the formation of multistability, which is common for a wide class of systems. Recently synchronization in a ring of three repulsively coupled phase oscillators has been reported [45]. The authors showed that few synchronization regimes can coexist in the system. However, they do not carry out a bifurcation analysis to explain the presence of multistability. We expect that the bifurcations are similar to the ones presented in our paper and underlie the multistability observed in [45].

It must be noted that the problem of phase multistability has been studied in other papers, e.g., [46]. However, the systems considered in [46] (nonreduced system of mutually coupled van der Pol oscillators) and other publications [1,15–17,20,21,37,38] do not possess a Hopf bifurcation in the phase-reduced case.

ACKNOWLEDGMENTS

S.A. was supported by the Alexander von Humboldt Foundation and the Federal Ministry of Education and Science of the Russian Federation (state Contract No. 14.740.11.0074). N.F. was supported by the Aihara Project, the FIRST program of the JSPS, initiated by CSTP. J.K. and N.F. were supported by FET Open Project SUMO (Grant No. 266722).

[1] Y. Kuramoto, *Chemical Oscillations, Waves, and Turbulence* (Springer-Verlag, New York, 1984).
[2] A. Pikovsky, M. Rosenblum, and J. Kurths, *Synchronization: A Universal Concept in Nonlinear Science* (Cambridge University Press, Cambridge, UK, 2001).
[3] D. Mertens and R. Weaver, Phys. Rev. E **83**, 046221 (2011).
[4] A. Feoktistov, S. Astakhov, and V. Anishchenko, *17th International Workshop on Nonlinear Dynamics of Electronic Systems* (Rapperswil, Switzerland, 2009), pp. 114–117.
[5] A. Neiman, X. Pei, D. Russell, W. Wojtenek, L. Wilkens, F. Moss, H. A. Braun, M. T. Huber, and K. Voigt, Phys. Rev. Lett. **82**, 660 (1999).
[6] A. Neiman, L. Schimansky-Geier, A. Cornell-Bell, and F. Moss, Phys. Rev. Lett. **83**, 4896 (1999).
[7] P. Tass, M. G. Rosenblum, J. Weule, J. Kurths, A. Pikovsky, J. Volkmann, A. Schnitzler, and H.-J. Freund, Phys. Rev. Lett. **81**, 3291 (1998).
[8] M. Wickramasinghe and I. Z. Kiss, Phys. Rev. E **83**, 016210 (2011).
[9] C. Zhou, J. Kurths, I. Z. Kiss, and J. L. Hudson, Phys. Rev. Lett. **89**, 014101 (2002).
[10] G. S. Duane and J. J. Tribbia, Phys. Rev. Lett. **86**, 4298 (2001).
[11] D. Maraun and J. Kurths, Geophys. Res. Lett. **32**, L15709 (2005).
[12] I. I. Mokhov, D. A. Smirnov, P. I. Nakonechny, S. S. Kozlenko, E. P. Seleznev, and J. Kurths, Geophys. Res. Lett. **38**, L00F04 (2011).
[13] M. McDonald, O. Suleman, S. Williams, S. Howison, and N. F. Johnson, Phys. Rev. E **77**, 046110 (2008).
[14] W.-X. Wang, X. Ni, Y.-C. Lai, and C. Grebogi, Phys. Rev. E **83**, 011917 (2011).
[15] H. Sakaguchi and Y. Kuramoto, Prog. Theor. Phys. **76**, 576 (1986).
[16] H. Daido, Physica D: Nonlin. Phenom. **91**, 24 (1996).
[17] H. Chiba and I. Nishikawa, Chaos **21**, 043103 (2011).
[18] P. Ashwin, O. Burylko, and Y. Maistrenko, Physica D: Nonlin. Phenom. **237**, 454 (2008).
[19] P. Ashwin, O. Burylko, Y. Maistrenko, and O. Popovych, Phys. Rev. Lett. **96**, 054102 (2006).
[20] J.-N. Teramae and D. Tanaka, Phys. Rev. Lett. **93**, 204103 (2004).
[21] I. Z. Kiss, C. G. Rusin, H. Kori, and J. L. Hudson, Science **316**, 1886 (2007).
[22] V. Anishchenko, T. Vadivasova, D. Postnov, and M. Safonova, Int. J. Bifurcat. Chaos **2**, 633 (1992).
[23] H. Fujisaka and T. Yamada, Prog. Theor. Phys. **69**, 32 (1983).
[24] L. M. Pecora and T. L. Carroll, Phys. Rev. Lett. **64**, 821 (1990).
[25] M. G. Rosenblum, A. S. Pikovsky, and J. Kurths, Phys. Rev. Lett. **76**, 1804 (1996).
[26] J. Lehnert, T. Dahms, P. Hövel, and E. Schöll, Europhys. Lett. **96**, 60013 (2011).
[27] I. Omelchenko, Y. Maistrenko, P. Hövel, and E. Schöll, Phys. Rev. Lett. **106**, 234102 (2011).
[28] A. A. Temirbayev, Z. Z. Zhanabaev, S. B. Tarasov, V. I. Ponomarenko, and M. Rosenblum, Phys. Rev. E **85**, 015204 (2012).
[29] A. A. Selivanov, J. Lehnert, T. Dahms, P. Hövel, A. L. Fradkov, and E. Schöll, Phys. Rev. E **85**, 016201 (2012).
[30] A. Bergner, M. Frasca, G. Sciuto, A. Buscarino, E. J. Ngamga, L. Fortuna, and J. Kurths, Phys. Rev. E **85**, 026208 (2012).
[31] N. Fujiwara and J. Kurths, Eur. Phys. J. B **69**, 45 (2009).
[32] N. Fujiwara, J. Kurths, and A. Díaz-Guilera, Phys. Rev. E **83**, 025101(R) (2011).
[33] N. Fujiwara, J. Kurths, and A. Díaz-Guilera, AIP Conf. Proc. **1389**, 1015 (2011).
[34] E. M. Izhikevich, SIAM J Appl. Math. **59**, 2193 (1999).

[35] V. Anishchenko, S. Nikolaev, and J. Kurths, Phys. Rev. E **73**, 056202 (2006).
[36] V. Anishchenko, S. Nikolaev, and J. Kurths, Phys. Rev. E **76**, 046216 (2007).
[37] V. Anishchenko, S. Astakhov, and T. Vadivasova, Europhys. Lett. **86**, 30003 (2009).
[38] V. Anishchenko, S. Nikolaev, and J. Kurths, Chaos **18**, 037123 (2008).
[39] Z. Levnajić and B. Tadić, Chaos **20**, 033115 (2010).
[40] Z. Levnajić, Phys. Rev. E **84**, 016231 (2011).
[41] J. Hasty, D. McMillen, and J. J. Collins, Nature **420**, 224 (2002).
[42] T. S. Gardner, C. R. Cantor, and J. J. Collins, Nature **403**, 339 (2000).
[43] M. B. Elowitz and S. Leibler, Nature **403**, 335 (2000).
[44] 'XPP/XPPAUT; http://www.math.pitt.edu/∼bard/xpp/xpp.html.
[45] M. Giver, Z. Jabeen, and B. Chakraborty, Phys. Rev. E **83**, 046206 (2011).
[46] A. G. Balanov, N. B. Janson, V. V. Astakhov, and P. V. E. McClintok, Phys. Rev. E **72**, 026214 (2005).